European Review for Medical and Pharmacological Sciences 2023; 27: 4718-4734

Pregnenolone protects the liver against doxorubicin-induced cellular injury by anti-inflammatory, antioxidant, and antiapoptotic mechanisms: role of Keap1/Nrf2/HO-1 and P-glycoprotein

M.A. MORSY[1,2], M. EL-DALY[3], B.A. KAMEL[4], R.A. RIFAAI[5], S.A. ABDEL-GABER[2]

[1]Department of Pharmaceutical Sciences, College of Clinical Pharmacy, King Faisal University, Al-Ahsa, Saudi Arabia
[2]Department of Pharmacology, Faculty of Medicine, Minia University, El-Minia, Egypt
[3]Department of Pharmacology and Toxicology, Faculty of Pharmacy, Minia University, El-Minia, Egypt
[4]Department of Biochemistry, Faculty of Medicine, Minia University, El-Minia, Egypt
[5]Department of Histology and Cell Biology, Faculty of Medicine, Minia University, El-Minia, Egypt

Abstract. – OBJECTIVE: Doxorubicin (DOX) is a widely used cytotoxic anthracycline antibiotic characterized by increased adverse effects that limit its clinical usefulness. Pregnenolone is a pregnane X receptor (PXR) agonist that increases the expression of xenobiotic transporters with anti-inflammatory and antioxidant potential. Thus, we hypothesized that pregnenolone would protect against DOX-induced hepatotoxicity.

MATERIALS AND METHODS: Male Wistar rats (180-200 g) were randomized into four groups (n = 7): Control, Control + Pregnenolone (35 mg/kg/day, orally), DOX (15 mg/kg, i.p.) single dose on day five, and Pregnenolone + DOX. All treatments continued for seven consecutive days. Twenty-four hours after the last treatment, serum and liver tissues were collected for biochemical and histopathological assessment. The possible interaction between pregnenolone and DOX on cell viability was tested in HepG2 cells *in vitro* by 3-(4,5-dimethylthiazol-2-yl)-2,5-diphenyltetrazolium bromide (MTT) assay.

RESULTS: DOX treatment resulted in hepatic damage and fibrosis with increased serum alanine aminotransferase (ALT) and aspartate aminotransferase (AST). Liver samples of the DOX-treated group showed increased oxidative stress [malondialdehyde (MDA) and total nitrite/nitrate and decreased reduced glutathione (GSH) and superoxide dismutase (SOD)], increased hepatic tumor necrosis factor-alpha (TNF-α), interleukin-10 (IL-10), transforming growth factor-beta1 (TGF-β1), and mRNA of interleukin-1beta (IL-1β) and interleukin-6 (IL-6). Pretreating the rats with pregnenolone antagonized these DOX-induced effects. Moreover, pregnenolone upregulated the hepatic expression of Nrf2, heme oxygenase-1 (HO-1), and P-glycoprotein and decreased Keap1, opposing the effects of DOX. Moreover, pregnenolone prevented the DOX-induced activation and nuclear translocation of NFκB and increased cleaved caspase-3. Pregnenolone potentiated DOX-mediated cytotoxicity in HepG2 cells.

CONCLUSIONS: These results illustrate the protective effects of pregnenolone against DOX-induced hepatotoxicity without limiting its anticancer activity.

Key Words:
Pregnenolone, Doxorubicin, Hepatotoxicity, Nrf2, Caspase-3, P-glycoprotein.

Introduction

Doxorubicin (DOX) is a broad-spectrum anticancer of the anthracycline antibiotic family with wide therapeutic applications. It is used alone or combined with other drugs to treat solid tumors, including breast, gastric, muscular, and thyroid cancers and hematological malignancies[1,2]. DOX is an essential component of clinically used chemotherapy regimens, including CHOP (cyclophosphamide, DOX, vincristine, and prednisone), R-CHOP (plus rituximab), EPOCH (prednisone, vincristine, cyclophosphamide, and DOX), and DA-EPOCH (with dose-adjusted etoposide), and others[3,4].

Like most anticancer agents, the high incidence of serious adverse effects limits the clinical benefits of DOX[5]. DOX induces dose-limiting cardiotoxic manifestations and severe myelosuppression that warrant a boxed warning on its packages[6]; however, it also harms other organs, such as the kidney and liver[7,8]. Thus, the search

Corresponding Author: Mohamed A. Morsy, Ph.D; e-mail: momorsy@kfu.edu.sa

for protective therapies against DOX-induced organ damage shall continue.

DOX undergoes extensive metabolic transformations in the liver by cytoplasmic and microsomal enzymes, with the hydroxylated metabolite doxorubicinol being the most toxic[5]. More than 50% of the DOX dose is usually excreted in feces. The accumulation of toxic intermediates in the hepatocyte mediates DOX-induced cellular injury[5,9,10]. The mechanisms underlying DOX-induced cytotoxicity include inducing DNA damage, increasing the production of reactive oxygen species (ROS), disrupting mitochondrial genes and metabolism, provoking inflammation, and activating cellular apoptosis[11,12]. The interplay between oxidative stress and inflammation to activate cellular apoptotic pathways is well-established in different disease models[11,13-15].

Increased cellular inflammation downregulates the expression of the cytoprotective carrier systems. Notable examples include the ATP-binding cassette (ABC) transporter P-glycoprotein (P-gp) – also known as multidrug resistance protein 1 (MDR1), which is encoded in humans by *ABCB1*, the multidrug resistance-associated protein 2 (MRP2)[16], and the multiple organic anion transporter proteins[17]. The activity of such transporters prevents the accumulation of harmful xenobiotics, hence protecting these cells against various insults. On the other hand, the upregulation of such transporters in tumor cells confers resistance against anticancer therapy[18,19].

Pregnenolone is a pregnane X receptor (PXR) agonist that stimulates the expression of liver microsomal enzymes, notably cytochrome P450 3A (CYP3A), ABC transporters, organic anion transporting polypeptides, glutathione transferases (GSTs), and UDP-glucuronosyl transferases (UGTs), thus antagonizing the inhibitory effects of increased inflammation on these factors[20-22]. Besides, the inflammation modulatory effects of pregnenolone have been reported[17,23,24]. Pregnenolone interferes with inflammatory gene transcription[25]. The reported antioxidant activity of pregnenolone, whether direct or based on its anti-inflammatory potential, adds another advantage[26,27].

Based on these pleiotropic effects of pregnenolone, we hypothesized that it would protect the liver against DOX-induced injury. We proposed that pregnenolone-mediated hepatoprotection would involve the activation of antioxidant, anti-inflammatory, and antiapoptotic signaling and upregulation of hepatic P-gp. To test this hypothesis, we pretreated experimental rats with or without pregnenolone before challenging them with a single hepatotoxic dose of DOX. We also tested the effect of combined pregnenolone and DOX on the proliferation of a hepatic cancer cell line *in vitro* to rule out the possible interaction between them.

Materials and Methods

Animals

Male Wistar rats of body weight 180-200 g from the National Research Center (NRC, Giza, Egypt) were kept under 25 ± 1°C and a 12-h light/dark cycle, with free access to standard animal chow and tap water. All experimental procedures were approved by the Faculty of Medicine-Research Ethics Committee, Minia University, Egypt (ethical approval No. 317/4/2022), following the EU directive 2010/63/EU.

Experimental Design

Following a one-week of acclimatization, animals were grouped into four groups (n = 7): 1) Control rats that received only the vehicle; 2) Control + Preg rats that received pregnenolone (pregnenolone carbonitrile, Cas Number: 1434-54-4, Toronto Research Chemicals, Toronto, Ontario, Canada) in a dose of 35 mg/kg/day, orally, dissolved in corn oil; 3) DOX rats that received a single i.p. DOX challenge (15 mg/kg) on day five, and 4) Preg + DOX rats that received both DOX and pregnenolone. All rats received the different treatments for seven consecutive days. On the fifth experiment day, DOX (dissolved in 0.9% saline) was injected intraperitoneally one hour after the routine daily treatment at 15 mg/kg in the DOX and Preg + DOX groups to induce hepatoxicity[7].

Sample Collection

All rats were euthanized after thiopental anesthesia (50 mg/kg, i.p.) 24-h after the last treatment to collect serum and liver tissues for biochemical and histopathological assessment. Briefly, blood collected by cardiac puncture was centrifuged at 5,000 rpm for 10 min after its coagulation for collecting the serum. The liver was immediately harvested, washed with cold saline, blotted dry on filter paper, and cut into portions. A piece of liver tissue from each rat was fixed in 10% neutral buffered formalin and further processed for histopathological and immunohistochemical staining[13,28]. Samples from each animal were submerged in RNA safeguard Reagent (Cat. No. BSC54M1, BioFlux, Bioer Technology, Hangzhou, China), kept at −80°C, and used later for

RNA extraction. The remaining portions of the liver tissue were homogenized in 10 mM ice-cold phosphate buffer (pH 7.4) to produce 10% w/v homogenates, which were centrifuged at 10,000 rpm for 10 min in a cooling centrifuge. The supernatants were stored at -80°C until used.

Determination of Liver Function and Redox State

Liver function was assessed by determination of the serum activity of alanine transaminase (ALT) and aspartate transaminase (AST) using commercial colorimetric kits (Biodiagnostic, Giza, Egypt) as previously described[29]. Lipid peroxidation in liver homogenates was measured at 534 nm as malondialdehyde (MDA) after a reaction with thiobarbituric acid[30]. The hepatic content of reduced glutathione (GSH) and superoxide dismutase (SOD) was determined, as previously reported[13,31]. Determination of the tissue nitric oxide (NO) output was measured as the total nitrite/nitrate (NOx) after reducing nitrate to nitrite using copper-coated cadmium beads. The absorbance of the colored product developed after reacting the Griess reagent with nitrite ions in the sample in an acid medium was used to calculate the total NO in each sample as described before[29].

Determination of Hepatic TNF-α and IL-10

The levels of hepatic tumor necrosis factor-alpha (TNF-α) and interleukin-10 (IL-10) were measured in the tissue homogenate supernatants for all groups using ELISA kits. The rat TNF-α (ab100785) and IL-10 (ab100765) ELISA kits (Abcam, Cambridge, United Kingdom) were used as per the manufacturer's recommendations[32].

Real-Time PCR Determination of IL-1β and IL-6 Gene Expression

Extraction of total RNA from liver tissues using the RiboZol Reagent (AMRESCO, Solon, OH, USA) was followed by a reverse transcriptase polymerase chain reaction (PCR) in the presence of non-specific primers to generate cDNA templates. cDNA templates (250 ng) of each sample were mixed with specific primers (1 μM) for interleukin-1beta (IL-1β): 5'-CAC CTT CTT TTC CTT CAT CTT TG-3' (sense) & 5'-GTC GTT GCT TGT CTC TCC TTG TA-3' (anti-sense); IL-6: 5'-TGA TGG ATG CTT CCA AAC TG-3'(sense) & 5'-GAG CAT TGG AAG TTG GGG TA-3' (anti-sense); and GAPDH: 5'-GTC GGT GTG AAC GGA TTT G-3' (sense) & 5'-CTT GCC GTG GGT AGA GTC AT-3'(anti-sense). The HERA SYBR green RT-qPCR kit was used to prepare the final reaction volume of 20 μL. The reaction was initiated and monitored in the StepOne™ Real-Time PCR Detection System (Applied Biosystems, Foster City, CA, USA). The expression of IL-1β and IL-6 genes was calculated relative to GAPDH in each sample[33].

Western Blot Analysis of Hepatic P-gp, TGF-β1, Keap1, Nrf2, and HO-1

Liver tissue supernatants containing 50 μg total protein were denatured (3 min at 95°C) in 2X sample buffer containing 2-mercaptoethanol and subjected to sodium dodecyl sulfate-polyacrylamide gel electrophoresis (SDS-PAGE)[34]. The separated protein bands were transferred to polyvinylidene fluoride (PVDF) membranes, which were blocked for 1 h by 5% non-fat milk and 0.05% Tween-20 in Tris-buffered saline (TBS-T). The membranes, after washing three times with TBS-T, were incubated overnight at 4°C with 1:1000 aliquots of primary immunoglobulins against P-gp (ab170904, Abcam, Cambridge, MA, USA), transforming growth factor-beta1 (TGF-β1) (ab215715, Abcam), Keap1 (ab227828, Abcam), Nrf2 (ab92946, Abcam), heme oxygenase-1 (HO-1) (ab52947, Abcam), histone H3 (ab1791, Abcam), or β-actin (ab115777, Abcam). Secondary goat anti-rabbit polyclonal antibodies (1:5000) tagged with horseradish peroxidase (Cell Signaling Technology, Danvers, MA, USA) in blocking buffer was applied for 1 h, and then washed three times. The specific protein bands were visualized by chemiluminescence, normalized to β-actin, or histone H3 (for Nrf2), and quantified as fold change relative to the normal control group with the help of Image J, version 1.53c (http://rsbweb.nih.gov/ij/; NIH, Bethesda, MD, USA)[35].

Histopathology and Immunohistochemistry

Paraffin-embedded hepatic tissue sections (5 μm thick) were subjected to hematoxylin and eosin (H&E) or Masson trichrome staining for determination of tissue morphological, or fibrotic changes, respectively, as described elsewhere[13,28,36]. Liver fibrotic changes were given a score of 0, 1, 2, 3, or 4 if showing: normal tissue, collagen deposits without septa, incomplete septa, complete but thin interconnected septa, or complete thick interconnected septa formation, respectively[37].

For immunohistochemical detection of tissue cleaved caspase-3 and NFκB, deparaffinized liver sections were rehydrated, washed with phosphate

buffered saline (PBS), and treated with H_2O_2 (3%) to block the activity of the endogenous peroxidase. After heat-activated antigen retrieval and blocking non-specific binding, primary antibodies were applied for NFκB-p65 or cleaved caspase-3 (cat. No. PA5-17264 and PA5-23921, respectively, ThermoFisher Scientific, Waltham, MA, USA) according to the supplier's recommendations. Following that, sections were treated for 0.5 h at room temperature with a peroxidase-conjugated secondary antibody. Protein expression was marked by the color developed after addition of 3,3′-diaminobenzidine (DAB), and sections were counterstained with hematoxylin[33]. A pathologist unaware of the experimental groups used ImageJ software[35] to measure the surface area fractions showing positive anti-NFκB-p65 or anti-cleaved caspase-3 staining.

Cell Viability Assay

The HepG2 liver cancer cells were used for the cell viability assay. Cell survival was assessed using the 3-(4,5-dimethylthiazol-2-yl)-2,5-diphenyltetrazolium bromide (MTT) method, as previously described[33]. Briefly, HepG2 liver cancer cells were subcultured initially at 10^4 cells/well in a 96-well plate for one day in DMEM. For another 24 h, the cells received DOX at 0.0, 0.1, 1, and 10 μM; pregnenolone at 0.1, 1, 10, or 100 μM; or their combinations. The MTT reagent (5 mg/mL in PBS) was then added (15 μL) to each well and incubated in the dark (37°C) for another 4 h. The formed formazan crystals were dissolved by adding dimethyl sulfoxide (100 μL) to each well. The absorbance at 540 nm was measured in a microplate reader.

Statistical Analysis

The results of different measurements are presented as mean ± SEM. The GraphPad Prism version 8.0.0 for Windows (GraphPad Software, San Diego, CA, USA) was used for data analysis. One-way analysis of variance (ANOVA) and Tukey's post-hoc test were used to compare different group means. The MTT assay cell survival data were analyzed using non-linear regression. Differences were considered significant when the *p*-value was lower than 0.05.

Results

Pregnenolone Ameliorates DOX-Induced Hepatotoxicity in Rats

Administration of 15 mg/kg DOX in male Wistar rats induced hepatic tissue damage, as shown in the H&E-stained sections (Table I and Figure 1). Examination of histopathological sections of groups 1 and 2 revealed normal hepatic architecture with the central veins and cords of hepatocytes radiating from them. The cords were separated by blood sinusoids. Hepatocytes appeared polyhedral with slightly acidophilic cytoplasm and vesicular nuclei. Portal tract areas showed branches of the hepatic artery, portal vein, and bile duct (Figure 1A-B). The DOX group showed abnormal hepatic architecture with congested central veins and dilated congested sinusoids. Besides, the portal areas showed marked inflammatory cell infiltration. Hepatocytes assumed apoptotic morphology with dense acidophilic cytoplasm and pyknotic nuclei. The latter effect was evident, especially in the periportal areas (Figure 1C1-C3). Meanwhile, sections from group 4, showed marked improvement. Both central veins and hepatic sinusoids appeared normal. Still, periportal inflammatory cell infiltration and scattered apoptotic hepatocytes were noticed (Figure 1D1-D3). Data in Table I summarize the injury scores in different groups.

Table I. Hepatic tissue microscopic injury scores.

	Control	Preg	DOX	Preg + DOX
Congestion	0	0	3	1
Hepatocyte apoptosis	1	1	3	2
Sinusoidal dilatation	0	0	3	1
Central vein dilatation	0	0	2	1
Periportal inflammation	0	0	3	2

Preg: pregnenolone; DOX: doxorubicin.

In line with the histology results, the untreated DOX group showed deteriorated liver function in comparison with the vehicle-treated controls. DOX-treated rats showed significantly higher serum activity of ALT and AST, which was ameliorated by pregnenolone pretreatment (Figure 2). However, the pregnenolone-treated DOX-intoxicated rats still showed higher than normal levels of serum liver function parameters.

Pregnenolone Improves DOX-Induced Hepatic Oxidative Stress

To study the role of oxidative stress in DOX-induced liver toxicity, we determined hepatic tissue levels of MDA, a marker of lipid per-

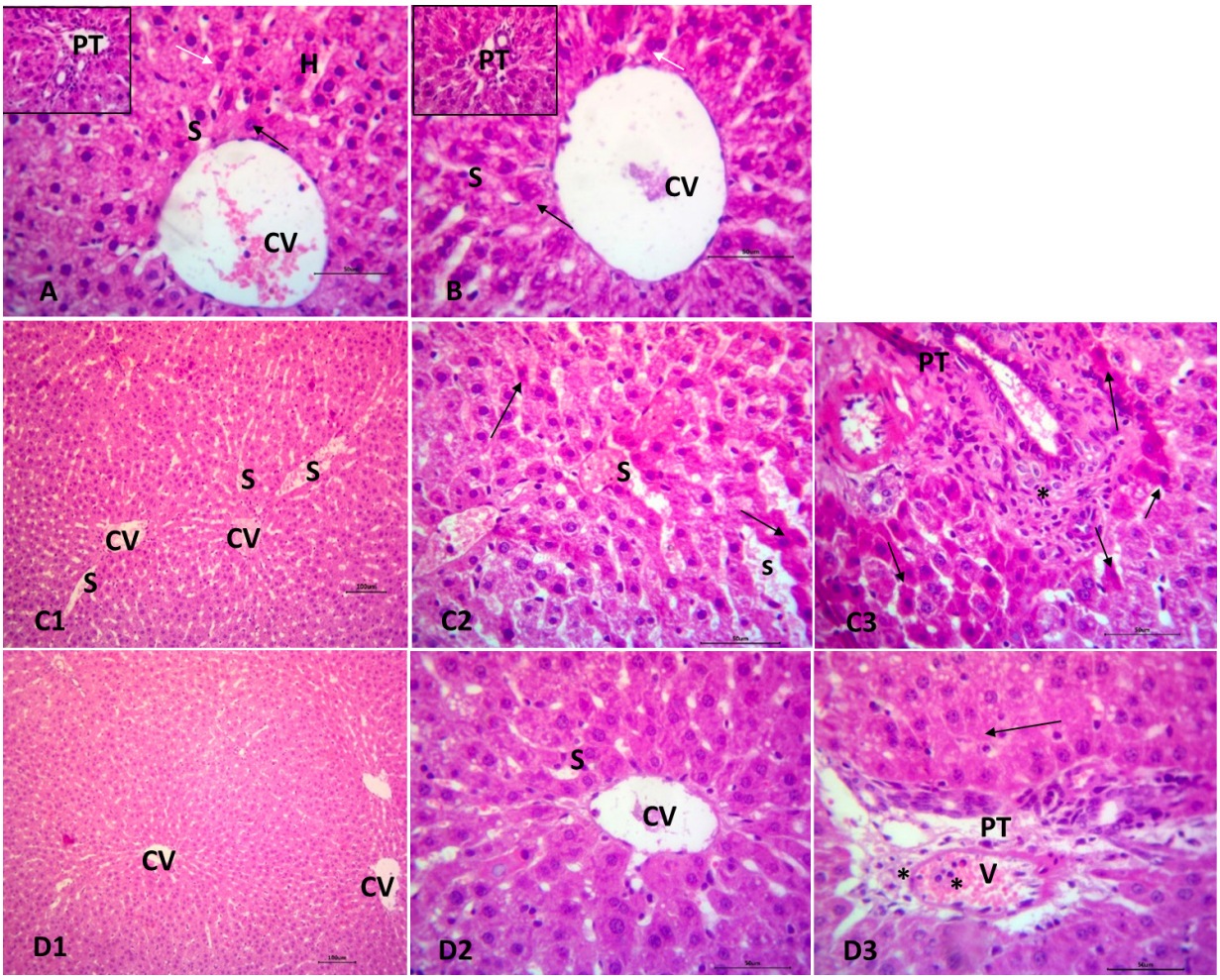

Figure 1. Pregnenolone protects against doxorubicin-induced hepatic tissue injury. Liver tissues were fixed in formalin and processed for H&E staining as described under Materials and Methods. **A-B**, Photomicrographs of the liver of groups 1 (untreated controls) and 2 (pregnenolone-treated) showing cords of hepatocytes (H). The hepatocytes appear with central vesicular nuclei (arrows), and some scattered hepatocytes are binucleated (white arrows). Notice the central vein (CV) and normal blood sinusoids (S). Insets show the portal tract (PT) area. H&E, ×400; scale bar = 50 µm. **C1-C3**, Photomicrographs of the liver of doxorubicin-treated rats showing markedly congested central veins (CV) and dilated congested sinusoids (S). Notice some apoptotic hepatocytes with dense acidophilic cytoplasm and pyknotic nuclei (arrows). **C3**, Shows the portal tract (PT) area with marked inflammatory cell infiltration (*) and many apoptotic hepatocytes with dense acidophilic cytoplasm and pyknotic nuclei (arrows). H&E, C1 ×100, (**C2, C3**) ×400; (**C1**) scale bar = 100 µm, (**C2, C3**) scale bar = 50 µm. **D1-D3**, photomicrographs of the liver of group 4 rats (treated with pregnenolone before induction of hepatotoxicity by doxorubicin) showing normal central veins (CV) and sinusoids (S). Notice the fewer apoptotic hepatocytes with dense acidophilic cytoplasm and pyknotic nuclei (arrow). **D3**, Shows portal tract (PT) area with some inflammatory cell infiltration (*) and normal periportal hepatocytes (arrow). H&E, D1 ×100, (**D2, D3**) ×400; (**D1**) scale bar = 100 µm, (**D2, D3**) scale bar = 50 µm.

oxidation, and total NOx content (Figures 3A-B). Compared with the control group, we observed a 3-fold increase in MDA and total NOx in the hepatic tissues of the untreated DOX group, which was completely abrogated when rats received pregnenolone pretreatment. We further studied the effect of DOX on hepatic SOD activity and levels of GSH. Tissues from DOX-treated rats showed normal SOD activity comparable to that of the normal control animals. However, pregnenolone treatment significantly increased hepatic SOD when compared with Control, DOX, or Preg + DOX groups (Figure 3C). Moreover, the liver of Preg + DOX rats showed significantly ($p < 0.5$) higher levels of SOD than the untreated DOX group. On the other hand, the DOX rats showed the lowest levels of GSH compared with all other groups. Importantly, pregnenolone-pretreated DOX rats showed normalized GSH levels (Figure 3D).

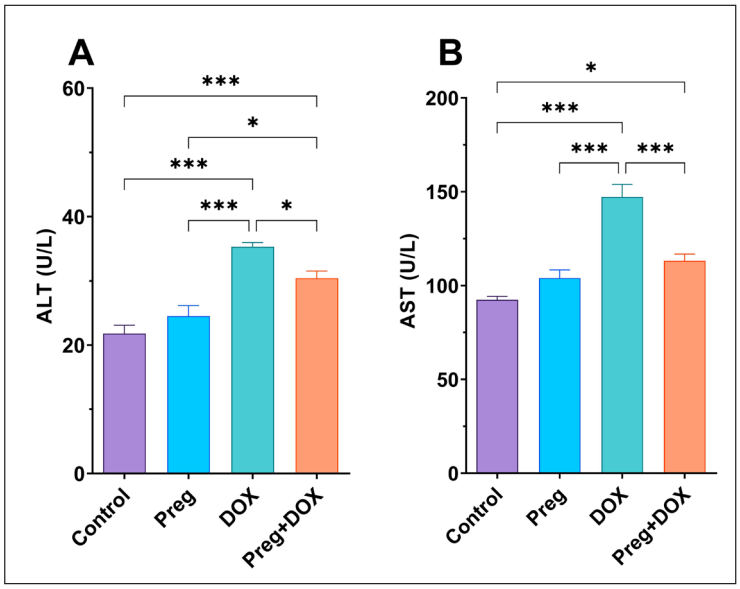

Figure 2. Pregnenolone (Preg) ameliorates doxorubicin (DOX)-induced elevation of ALT and AST. The activity of serum ALT (**A**) and AST (**B**) were measured spectrophotometrically as markers of liver function. Animals received only vehicle (Control), Preg (35 mg/kg/day, p.o.), DOX (15 mg/kg), or Preg + DOX. All treatments continued once daily for seven days except for DOX, which was administered only once on the fifth day of the experiment. Data, represented by the mean ± SEM of 6-7 observations, were analyzed by one-way ANOVA followed by Tukey's test for multiple comparisons. *,***: denote significant differences between the assigned groups at *p*-values lower than 0.05 and 0.001, respectively.

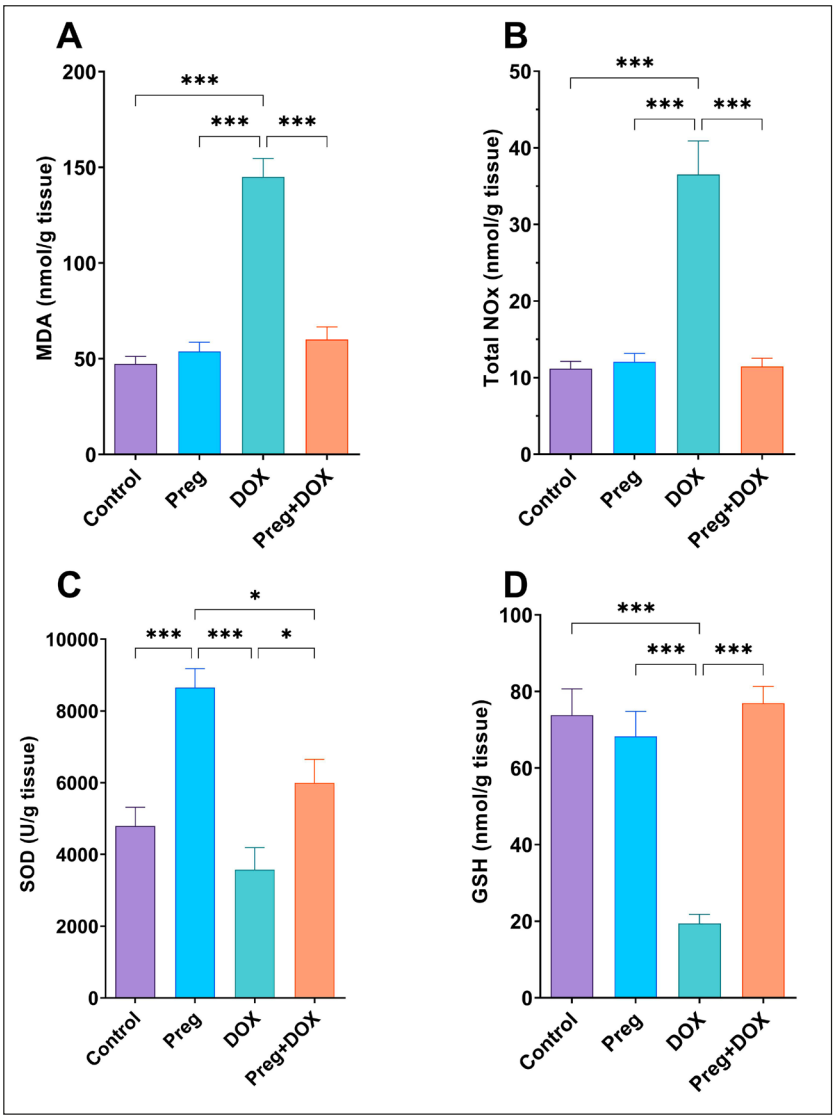

Figure 3. Pregnenolone (Preg) mitigates doxorubicin (DOX)-induced oxidative and nitrative stress. Rats were treated with vehicle (Control), Preg (35 mg/kg/day, p.o.), DOX (15 mg/kg), or Preg + DOX. All treatments were given once daily for seven days except for DOX, which was administered only once on the fifth day of the experiment. Liver tissues were homogenized, as described in Materials and Methods, and the supernatants from each group were used for the determination of (**A**) malondialdehyde (MDA), (**B**) total nitrite/nitrate (NOx), (**C**) activity of superoxide dismutase (SOD), and (**D**) reduced glutathione (GSH). Data, represented by the mean ± SEM of 6-7 observations, were analyzed by one-way ANOVA followed by Tukey's test for multiple comparisons. *,***: denote significant differences between the assigned groups at *p*-values lower than 0.05 and 0.001, respectively.

Pregnenolone Protects Against DOX-induced Liver Fibrosis

Using Masson trichrome staining, we tested the ability of pregnenolone to prevent liver fibrotic changes after the DOX challenge (Figure 4). Tissue sections from the control and pregnenolone groups showed normal collagen distribution within the hepatic lobules (grade 0, Figure 4A-B). Conversely, the collagen fibers significantly increased, and the fibrous septa were formed within the hepatic lobules of DOX-treated rats (Figure 4C). The fiber deposition was evident in the portal area and interconnected with the neighboring septa (grade 3). In the pregnenolone-treated DOX-challenged rats, hepatic collagen fibers decreased, and collagen distribution appeared normal (grade 0). In line with these findings, the DOX-intoxicated rats showed the highest hepatic levels of TGF-β1, which was partially ameliorated with pregnenolone pretreatment (Figure 4E).

Pregnenolone Protects Against DOX-Induced Liver Inflammation

Induction of liver tissue inflammation by DOX was evaluated by determining tissue levels of TNF-α and IL-10 and the gene expression of IL-1β and IL-6. DOX administration significantly increased hepatic TNF-α, which was partially ameliorated by pretreating the rats with pregnenolone (Figure 5A). Moreover, pregnenolone completely inhibited the DOX-induced induction of IL-1β and IL-6 (Figure 5B-C). On the other hand, the untreated DOX-challenged rat livers showed significantly elevated IL-10 compared with the vehicle- or pregnenolone-treated control groups. This increase was further augmented when DOX was combined with previous pregnenolone treatment (Figure 5D).

To confirm the DOX-activated inflammatory signaling in hepatic tissues, we investigated its effect on NFκB activation and its nuclear translocation by immunohistochemistry. The vehicle- and

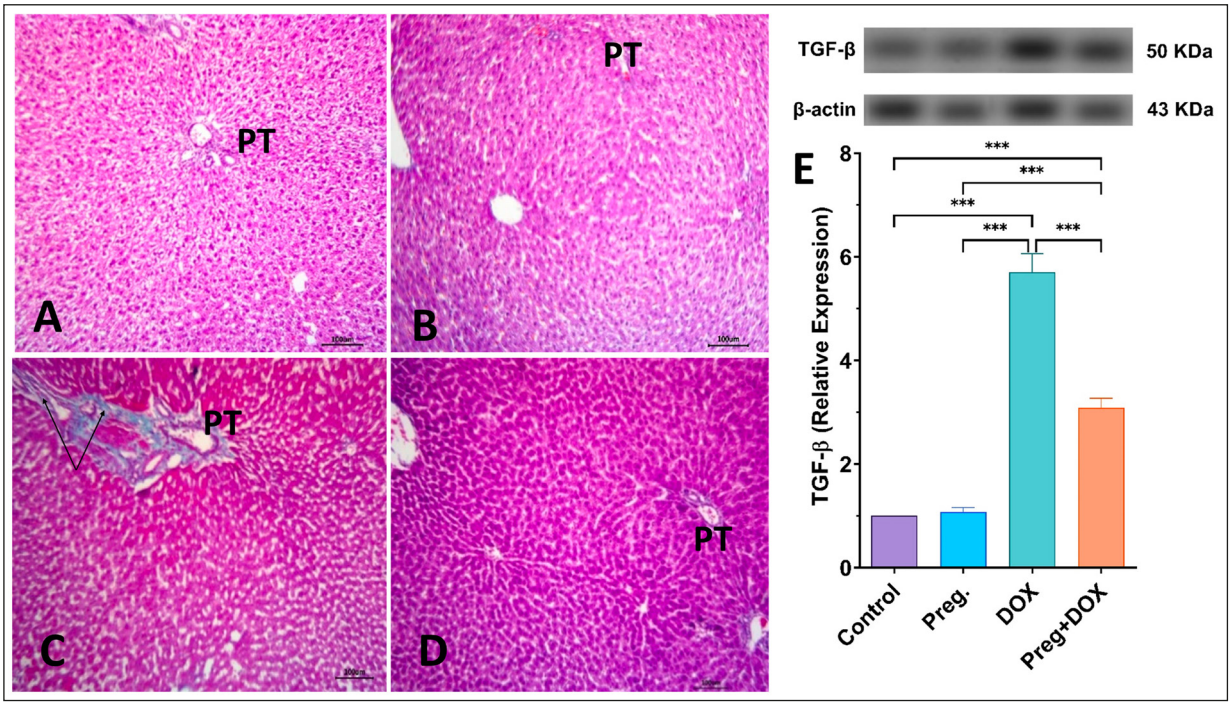

Figure 4. Pregnenolone (Preg) protects against doxorubicin (DOX)-induced hepatic fibrosis. Liver tissues were fixed in formalin and processed for Masson trichrome staining as described in Materials and Methods. Representative photomicrographs of the liver represent (**A**) Group 1 (untreated controls) and (**B**) Group 2 (Preg-treated), showing normal collagen distribution in the portal area (PT). **C**, A representative photomicrograph from Group 3 (DOX-treated) showing extensive collagen fiber depositions in the portal area (PT) and bridging between lobules (arrows). **D**, A representative photomicrograph from Group 4 shows normal collagen distribution in the portal area (PT). Masson trichrome, ×100, scale bar = 100 μm. **E**, Hepatic TGF-β1 levels were semi-quantified in tissue homogenates by Western blotting after SDS-PAGE of proteins, as described in Materials and Methods. Data (mean ± SEM) were analyzed by one-way ANOVA followed by Tukey's test for multiple comparisons. **,***: denote significant differences between the assigned groups at *p*-values lower than 0.01 and 0.001, respectively.

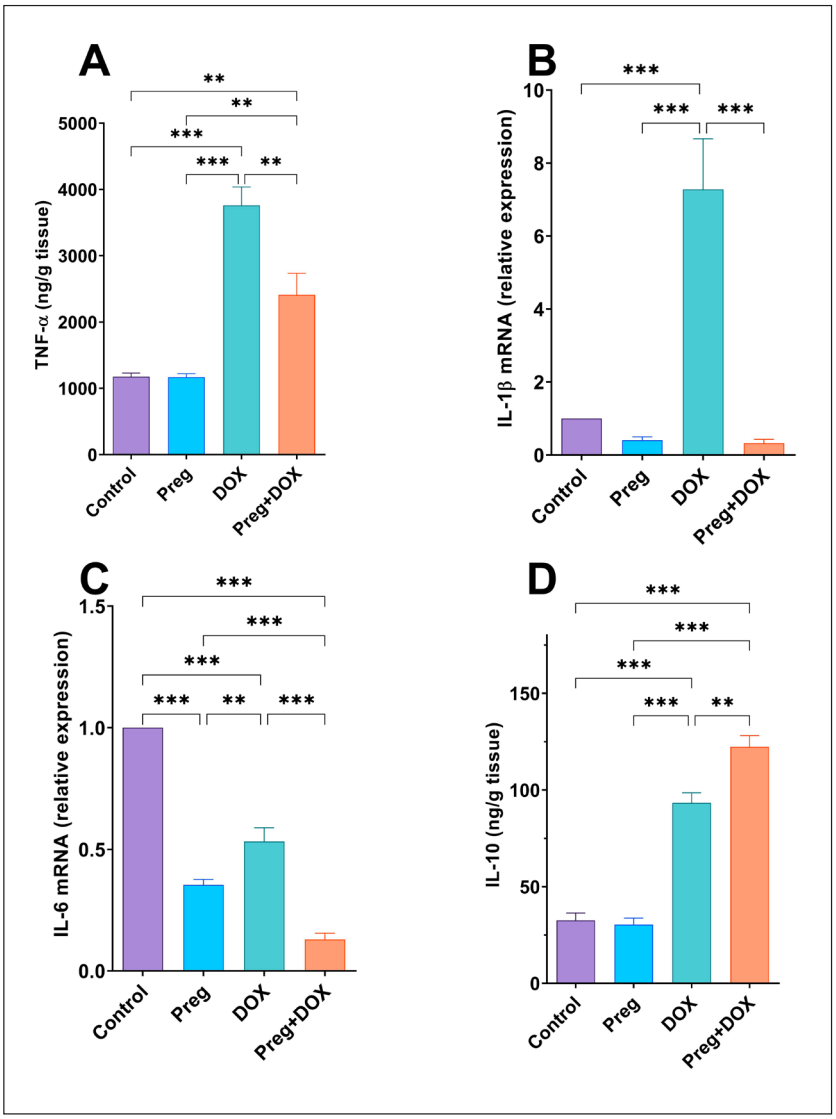

Figure 5. Pregnenolone (Preg) ameliorates doxorubicin (DOX)-induced liver inflammation. Rats in the Control, Preg, DOX, or Preg + DOX groups received the vehicle, Preg (35 mg/kg/day, p.o.), DOX (15 mg/kg), or Preg + DOX at the same dose levels, respectively. All treatments were given once daily for seven days except for DOX, which was administered only once on the fifth day of the experiment. Liver tissues were homogenized, as described in Materials and Methods, and the supernatants from each group were used for the determination of (**A**) TNF-α (ELISA), (**B**) IL-1β (real-time PCR), (**C**) IL-6 (real-time PCR), and (**D**) IL-10 (ELISA). The real-time PCR data were quantified relative to the expression of GAPDH. Data, represented by the mean ± SEM of 6-7 observations, were analyzed by one-way ANOVA followed by Tukey's test for multiple comparisons. **,***: denote significant differences between the assigned groups at *p*-values lower than 0.01 and 0.001, respectively.

pregnenolone-treated control groups showed negative hepatocyte staining for NFκB expression (Figure 6A-B). On the other hand, sections from the DOX group showed both pericentral and periportal hepatocytes with high positive cytoplasmic and nuclear expression (Figure 6C1-C2). Meanwhile, sections of the combined pregnenolone- and DOX-treated rats showed scattered hepatocytes with a faint positive cytoplasmic expression and significantly lower nuclear translocation of NFκB (Figure 6D).

Pregnenolone Protects Against DOX-Induced Activation of Apoptosis

As shown in Figure 7, hepatic tissues from the untreated or pregnenolone-treated control groups showed very low positivity for activated caspase-3 (Figure 7A-B). Contrarily, challenging the untreated rats with a single dose of DOX (15 mg/kg) increased the hepatic tissue reactivity towards anti-caspase-3 antibodies in the pericentral and periportal areas (Figure 7C-D). These proapoptotic effects of DOX were significantly mitigated by pretreating the rats with pregnenolone in Group 4 (Figure 7D-E).

Pregnenolone Protects Against DOX-Induced Hepatotoxicity by Modulating the Keap1/Nrf2/HO-1 Pathway and P-gp

To further understand the mechanisms by which pregnenolone protects the liver against DOX-induced inflammation and oxidative damage, we investigated the Keap1/Nrf2/HO-1 in tissue homogenates.

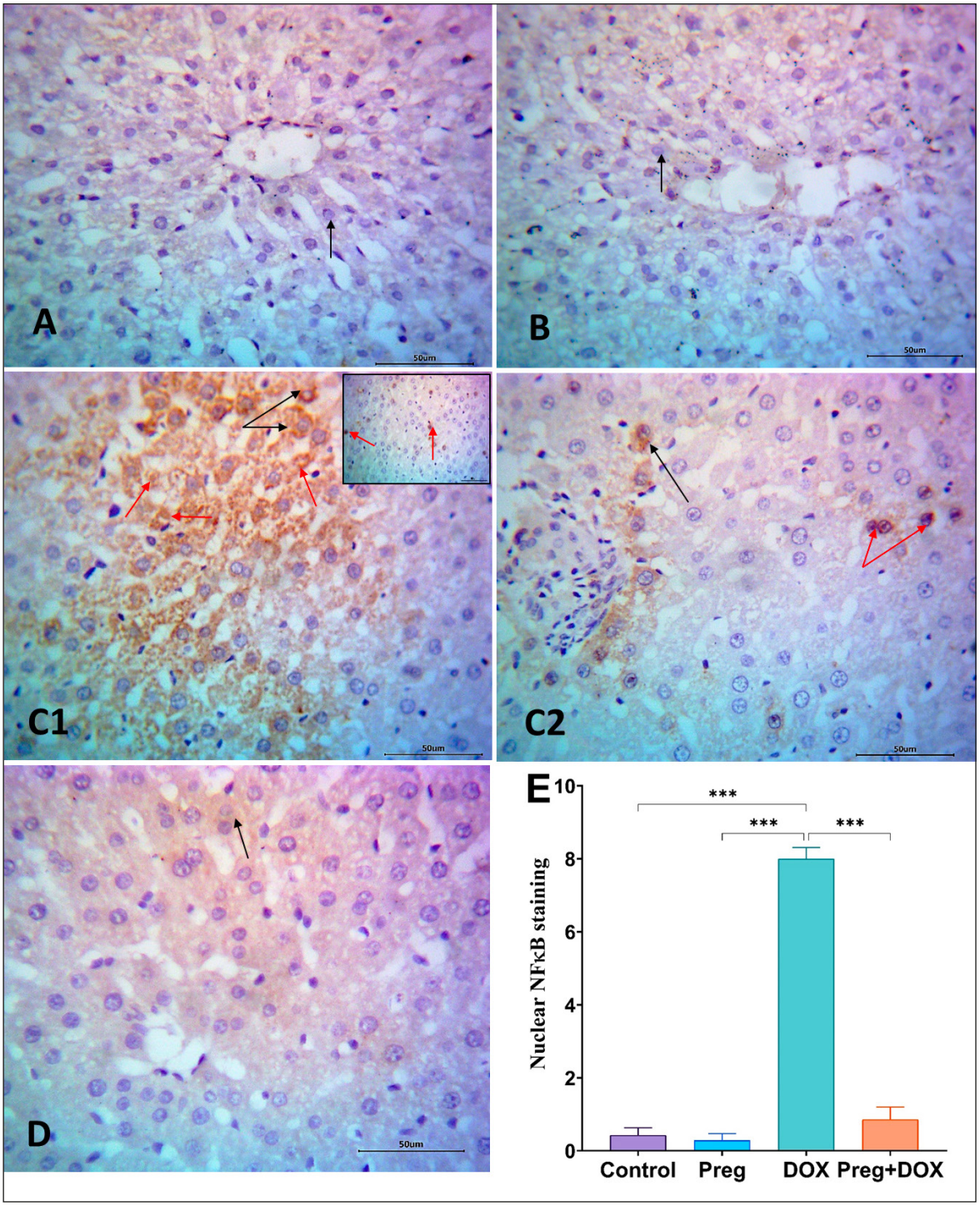

Figure 6. Pregnenolone (Preg) abolishes doxorubicin (DOX)-induced activation of NFκB. Hepatic tissues from different groups were stained after treatment with anti-NFκB, as described in detail in Material & Methods. Photomicrographs (**A, B**) represent the vehicle- and Preg-treated control rat livers showing negative NFκB expression (arrows). Photomicrographs (**C1, C2**) of tissues from the untreated DOX-challenged rats show strong hepatic expression of NFκB. (**C1**) Illustrates the pericentral hepatocytes with dense positive cytoplasmic (black arrows) and nuclear (red arrows) NFκB signal, which is also illustrated in the inset. Similarly, the periportal hepatocytes show positive cytoplasmic (black arrow) and nuclear expression (red arrows) (**C2**). **D**, A photomicrograph of the liver from Group 4 stained for NFκB shows faint expression in scattered hepatocytes (arrow). (CV) central vein, (PT) portal tract ×400, scale bar = 50 µm. **E**, Bar chart showing the number of positively stained brown nuclei in each group as counted in 7 non-overlapping fields (×400). Data, presented as the mean ± SEM, were analyzed by one-way ANOVA followed by Tukey's test for multiple comparisons. ***: denote significant differences between the assigned groups at *p*-values < 0.001.

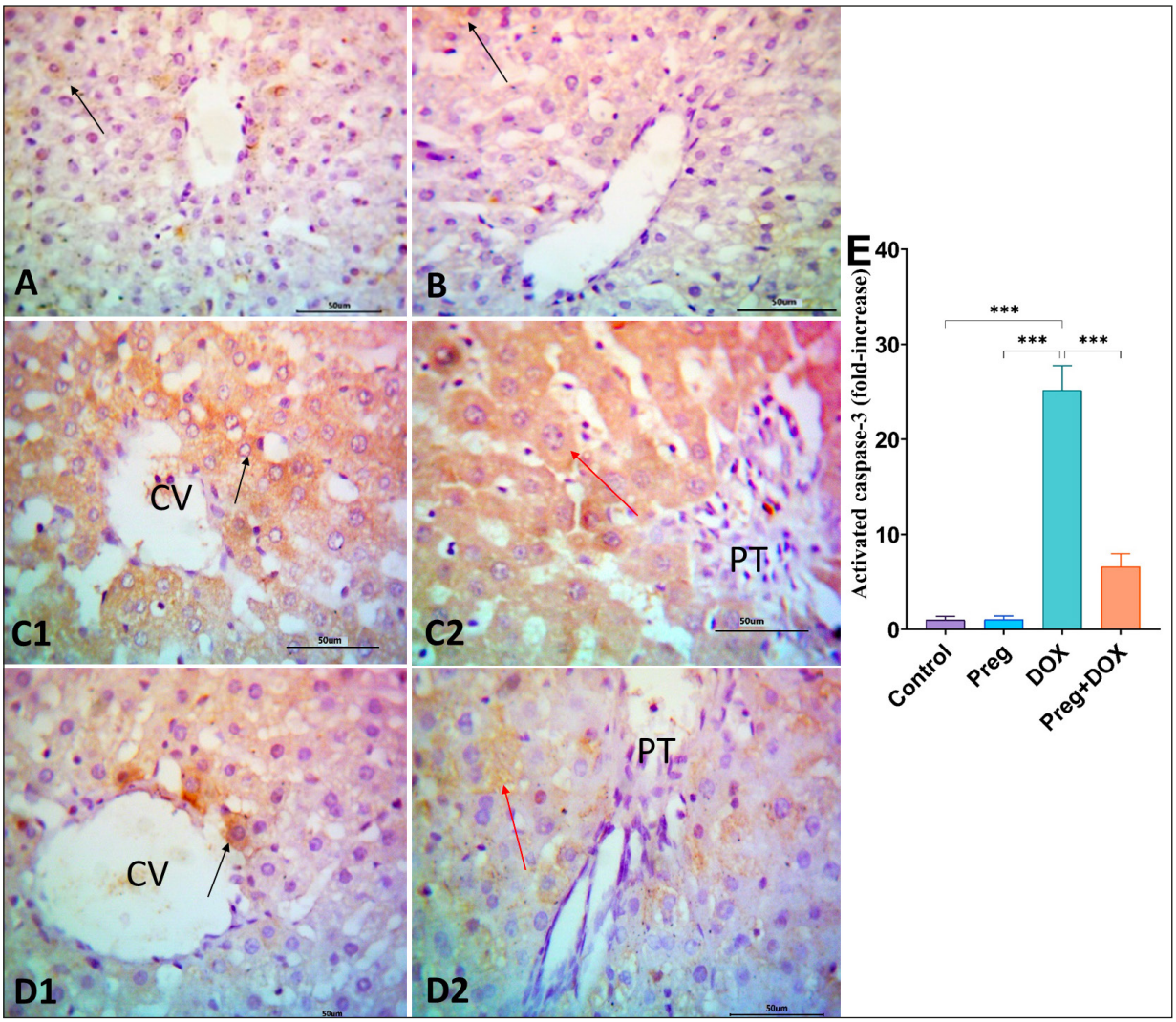

Figure 7. Pregnenolone (Preg) protects against doxorubicin (DOX)-induced proapoptotic effects. Tissue sections from different groups were stained for cleaved caspase-3. The representative photomicrographs of the liver tissue immunostained for active caspase-3 in (**A, B**) show negative expression in most of the hepatocytes from the vehicle-treated (**A**) and the Preg-treated (**B**) control groups; only a few scattered hepatocytes show faint expression (arrows). The photomicrographs (**C1, C2**) of Group 3 show high cytoplasmic expression of active caspase-3 in most of the precentral (black arrow) and periportal (red arrow) hepatocytes. Tissues from the Preg + DOX rats (**D1, D2**) show positive cytoplasmic expression in scattered hepatocytes both in the pericentral (black arrow) and periportal area (red arrow). (CV) central vein, (PT) portal tract ×400, scale bar = 50 µm. **E,** Bar chart showing the number of positively stained cells in each group as counted in 7 non-overlapping fields (×400). Data, presented as the mean ± SEM, were analyzed by one-way ANOVA followed by Tukey's test for multiple comparisons. ***: denote significant differences between the assigned groups at *p*-values < 0.001.

Challenging the experimental animals with a single large dose of DOX increased the protein levels of Keap1 (Figure 8A-E) while it decreased both Nrf2 and HO-1 (Figure 8B-C-E). Pregnenolone alone did not alter the expression of these proteins compared to the control vehicle-treated rats. On the other hand, the liver tissues of rats pretreated with pregnenolone before the DOX insult showed normalized levels of Keap1 and Nrf2. In addition, these Preg + DOX rats displayed significantly higher HO-1 than the untreated DOX rats. However, pregnenolone pretreatment in this group failed to normalize HO-1 expression (Figure 8C-E).

On the other hand, the DOX-intoxicated rats displayed significantly decreased P-gp levels compared with the normal expression observed in the vehicle- or pregnenolone-treated controls (Figure 8D-E). The DOX-induced decrease in hepatic P-gp was significantly mitigated when the rats were pretreated with pregnenolone before the DOX injection.

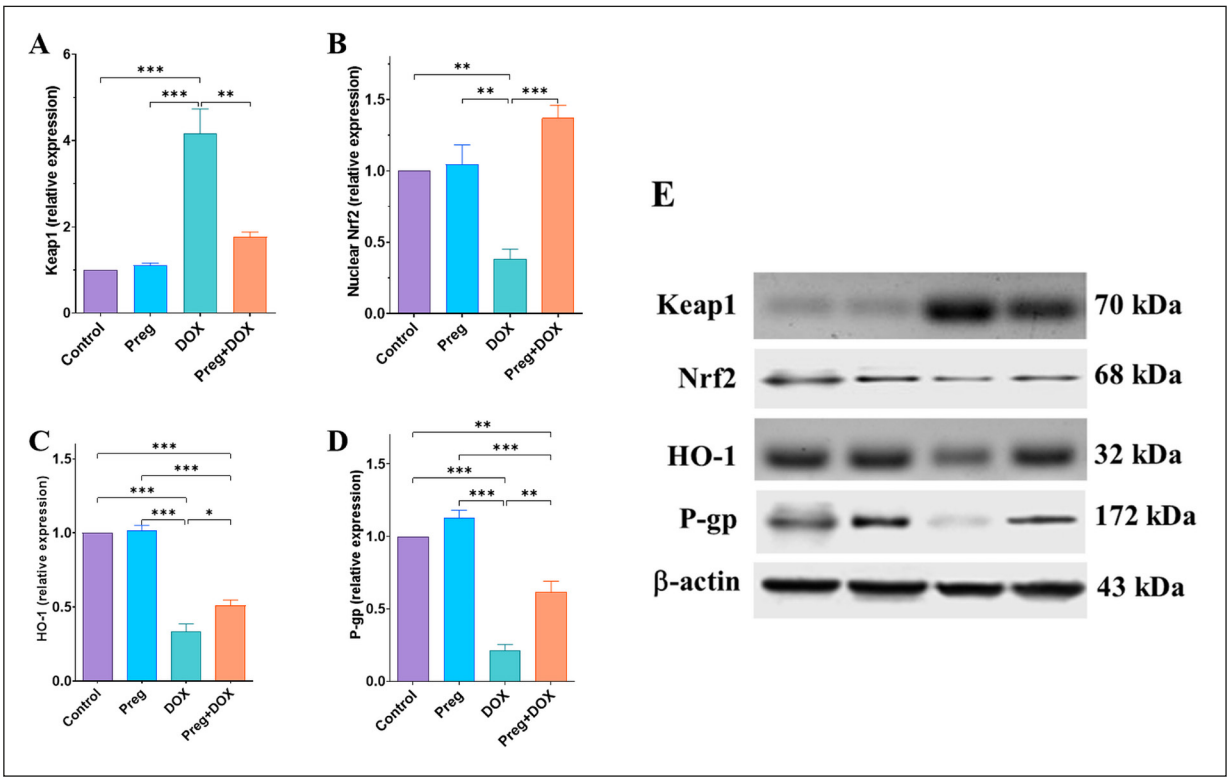

Figure 8. Effect of pregnenolone (Preg) pretreatment on doxorubicin (DOX)-induced modulation of hepatic Keap1, Nrf2, HO-1, and P-gp. Hepatic tissue homogenates were centrifuged, and proteins in the supernatants were separated by SDS-PAGE followed by blotting on PVDF membranes and probed with antibodies against Keap1 (**A**), Nrf2 (**B**), HO-1 (**C**), or P-gp (**D**) as described in detail in Materials and Methods. **E**, A representative western blot. Rats in the Control, Preg, DOX, or Preg+DOX groups received the vehicle, Preg (35 mg/kg/day, p.o.), DOX (15 mg/kg), or Preg + DOX at the same dose levels, respectively. All treatments were given once daily for seven days except for DOX, which was administered only once on the fifth day of the experiment. Data, represented by the mean ± SEM of three independent observations, were analyzed by one-way ANOVA followed by Tukey's test for multiple comparisons. *,**,***: denote significant differences between the assigned groups at $p < 0.05$, 0.01, and 0.001, respectively.

Pregnenolone Potentiates DOX-Induced Cytotoxicity In Vitro

To investigate the possibility that pregnenolone would antagonize the cytotoxic effects of DOX, we cultured HepG2 cells in the presence or absence of pregnenolone (0.0-100 μM), DOX (0.1-10 μM), or their combinations. DOX alone, incubated at 0.1, 1, and 10 μM, significantly reduced HepG2 survival by 19.6 ± 2.29, 28.7 ± 1.15, and 71.3 ± 1.27%, respectively (Figure 9, inset). On the other hand, pregnenolone treatment inhibited HepG2 survival by 11.7 ± 3.17 at 0.1 μM, 26.8 ± 3.85 at 1 μM, 41.2 ± 3.75 at 10 μM, and 45.5 ± 3.69 at 100 μM. Moreover, combining pregnenolone with DOX significantly potentiated the cytotoxic effects of DOX over the used concentration range (Figure 9, shaded box) compared with the respective DOX concentrations (first point in each red line). The best cytotoxic effects were achieved in cells treated with pregnenolone (100 μM) and DOX (10 μM).

Discussion

DOX is an essential component of the anticancer drug arsenal with multiple therapeutic applications[1,2]. However, the induction of serious adverse effects limits its clinical applications[5]. Although famous for inducing dose-limiting cardiotoxicity, DOX harms other organs, such as the liver[38-40]. The current study investigated the possible protection of pregnenolone against DOX-induced hepatotoxicity. A single high dose of DOX precipitated significant hepatic structural damage, as revealed by liver histology and confirmed by the increased serum markers of hepatotoxicity in the rats. Moreover, DOX-treated rats showed increased hepatic inflammation that paralleled fibrotic (increased collagen deposition) and proapoptotic (activation of caspase-3) changes. On the other hand, pregnenolone treatment protected the liver of DOX-intoxicated rats, improved

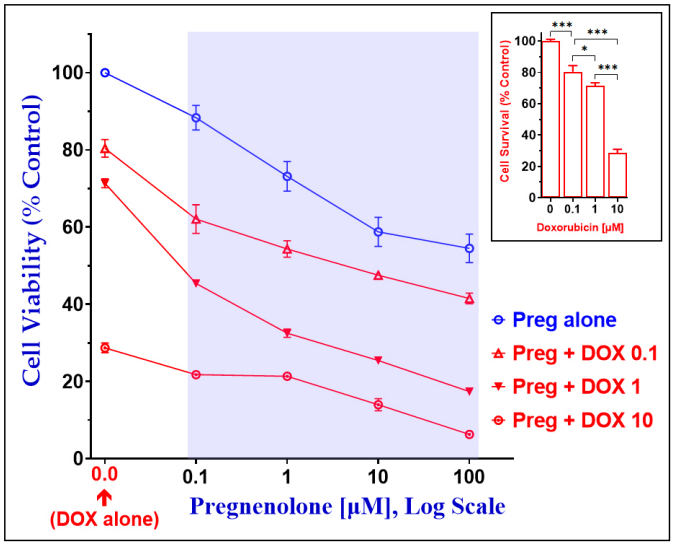

Figure 9. Pregnenolone (Preg) potentiates doxorubicin (DOX)-induced cytotoxicity in HepG2 cells. Hepatic HepG2 cells were cultured in DMEM with or without Preg (0.0-100 µM, blue line), DOX (0.1-10 µM, inset or each first point in the red lines), or combinations of both (red lines, shaded box). All treatments were continued for 24 h, followed by an MTT assay to measure cell survival. Data representing the mean ± SEM of three independent experiments were analyzed by one-way ANOVA followed by Tukey's test for multiple comparisons. *,***: denote significant differences between the assigned groups at $p <$ 0.05 and 0.001, respectively.

liver function parameters, and antagonized the DOX-induced inflammation. Besides, pregnenolone-treated rats showed conserved redox homeostasis, unlike the untreated DOX-challenged rats, which showed increased hepatic oxidative stress and diminished endogenous antioxidant defense.

Despite the increased detoxification capacity of the liver as compared with other tissues, previous studies[7,8,38,39] illustrated the inability of hepatocytes to overcome acute or chronic toxic DOX exposures. In hepatocytes, the microsomal enzymes metabolize DOX to produce the more toxic metabolite doxorubicinol, which can also occur in other tissues, such as the heart[5]. The mechanisms of DOX-induced cytotoxicity result from its cellular accumulation and subsequent DNA damage, induction of oxidative stress, and activation of inflammatory signaling[10-12,40-42]. Together, these actions might explain the failure of hepatocyte endogenous protective mechanisms, as illustrated by the current data.

Disruption of mitochondrial integrity and function and upregulation of ROS-mediated signaling is essential to the deleterious effects of DOX in normal cells, including the hepatocytes[7,8,10]. In the present study, a single high dose of DOX induction of hepatotoxicity increased tissue lipid peroxidation and total NOx and decreased the hepatic SOD activity and levels of GSH, indicating increased oxidative stress. Similar results have been previously reported for DOX-induced hepatotoxicity[8,10,43]. Others have shown the hepatoprotective effects of pregnenolone in acetaminophen-induced[44] and lithocholic acid-induced liver toxicity. Studies[26,27] in other disease models supported the antioxidant activity of pregnenolone, which might partly depend on its anti-inflammatory potential. Our results provide further evidence of the hepatoprotective effects of pregnenolone by preserving the redox homeostasis in the liver.

Increased cellular ROS, either under physiological conditions or after acute cellular insult, liberates Nrf2 from Keap1. Nrf2 then translocates to the nucleus and binds its antioxidant response element (ARE) to stimulate the transcription of antioxidant genes. This pathway is an essential switch in redox signaling and cellular homeostasis[7,10,45]. However, this antioxidant mechanism is compromised by DOX because of increased Nrf2 proteasomal degradation. Although the initial response to DOX involves destabilization of Keap1, hence the increased Nrf2 signaling[46], prolonged exposure destabilizes Nrf2 itself to enhance cellular oxidative stress[47]. Besides, the reductive metabolic transformation of DOX itself provokes superoxide generation. Apart from its direct toxic effects, superoxide is converted to hydrogen peroxide by the activity of SOD. In the presence of ferrous ions, hydrogen peroxide generates more damaging hydroxyl radicals[42]. This disruption of redox homeostasis was reported in DOX-induced cardiotoxicity[12,45] and hepatotoxicity[10,39,48,49].

The results of the current work showed upregulation of Keap1 and downregulation of Nrf2 proteins in the liver of DOX-treated rats, which accompanied the diminished expression of HO-1. Although some previous reports supported an immediate increase in Nrf2-dependent gene expression after acute DOX treatment, this effect was attributed to Keap1 degradation rather than

increased Nrf2 upregulation[46]. Moreover, research by the same group revealed that chronic exposure to DOX resulted in compromised Nrf2 and dependent genes[47]. Moreover, others reported disruption of Nrf2 expression and upregulated Keap1 after a single acute dose exposure *in vivo* and *in vitro*[50], which supports the current observations. In the study by Zhao et al[50], mice treated with 20 mg/kg DOX suffered from hepatotoxicity, which was explained by the decreased levels of Nrf2 and its target genes: HO-1 and NAD(P)H Quinone Dehydrogenase 1 (*Nqo1*). Importantly, these effects were mitigated by pregnenolone, which completely prevented the effect of DOX on Nrf2 and Keap1 and caused a modest, but significant, upregulation of HO-1.

Here, we tested the hypothesis that the hepatotoxic effects of DOX might be driven partly by the induction of inflammation. The correlation between ROS signaling, inflammation, and apoptosis is well-established[11,13-15]. The liver tissues from DOX-challenged rats manifested increased TNF-α protein and increased IL-6 and IL-1β gene activation, indicating enhanced inflammatory signaling. These findings are supported by the increased NFκB expression and nuclear translocation we found here. Our results align with previous reports[43,48,51] showing the role of inflammation in DOX-mediated toxicity. Nonetheless, the DOX-treated rats showed increased expression of IL-10 that was further augmented with pregnenolone treatment. The increase of this anti-inflammatory cytokine might be a compensatory mechanism as a result of tissue injury[52]. Recently, patients receiving liposomal DOX had higher serum levels of IL-10[53].

The current experiment results showed that DOX-induced liver injury increased hepatic collagen deposition and TGF-β1 expression indicating fibrotic changes. Besides, these tissues manifested elevated cleaved caspase-3, an apoptotic marker. These findings might help explain the histological tissue damage in DOX-treated rats. On the contrary, pregnenolone treatment antagonized these DOX-mediated effects. Oxidative stress and inflammatory signaling can activate liver fibrotic changes and proapoptotic mechanisms[14,37,51]. Moreover, the induction of tissue fibrosis and apoptosis is characteristic of DOX-induced hepatotoxicity[10,15,51,54]. Previous studies[55-58] reported the antifibrotic[55,56] and antiapoptotic[57,58] effects of pregnenolone. However, others reported proapoptotic effects of pregnenolone or its derivatives in primary cells and cancer cell lines[59-62].

Activation of inflammation limits the cellular capacity to extrude xenobiotics by decreasing the expression of cytoprotective transporters, such as P-gp (MDR1) and MRP2[16-18,22]. This effect of inflammation contributes to cell injury, as observed in the current study, and strongly correlates with the DOX-induced inflammatory signaling and its well-established organ toxicity. The DOX treatment dramatically decreased the hepatic expression of P-gp, which is in line with the structurally evident damage. Although these effects might potentiate anticancer activity in tumor cells, inflammatory signaling sensitizes normal cells toward the toxic effects of exogenous chemicals[18,19,33].

Although pregnenolone did not affect the expression of P-gp in control rats, it prevented the DOX-induced downregulation. This mechanism might contribute to the pregnenolone-mediated hepatoprotection by inhibiting DOX intracellular accumulation. We have recently shown that preservation of P-gp level confers protection against methotrexate-induced liver injury[33], which corroborates the present results. Moreover, the induction of a polymicrobial sepsis model in rats decreased the renal and pulmonary expression of P-gp, which was ameliorated by anti-inflammatory treatment[63].

By activating PXR, pregnenolone can stimulate hepatic detoxification mechanisms, including upregulation of P-gp. Other possible mechanisms include the upregulation of metabolizing enzymes such as CYP3A, GSTs, and UGTs[20-22]. Moreover, accumulating evidence illustrated the anti-inflammatory effects of pregnenolone *via* antagonizing signaling by cytokine and NFκB signaling[17,23,24]. These effects involve modulation of NFκB-mediated gene transcription and possibly non-genomic effects[25].

The cytotoxic potential of pregnenolone has been demonstrated in early experiments showing activation of retinal apoptotic cell death *in vitro* at 50 μM[60]. More recent work highlighted the cytotoxic potential of pregnenolone and its derivatives against the liver cancer cells HepG2 by downregulating Bcl-2[59]. However, given the observed pregnenolone-mediated cytoprotective effects against DOX-induced liver injury, notably the induction or preservation of P-gp, we asked whether it might protect cancer cells against the effects of DOX. We tested this possibility by assessing the cell viability of a liver cancer cell line, HepG2, in the absence and presence of pregnenolone either alone or combined with DOX. Our results showed that pregnenolone concentration-dependently potentiated the antiproliferative effects of DOX. Moreover, pregnenolone itself reduced HepG2

cell viability, especially at higher concentrations. These results are comparable to those observed by others[59] while studying the same cells. Further support for the current findings comes from other studies[61,62] highlighting the proapoptotic effects of pregnenolone and its derivatives.

Conclusions

Pregnenolone protected the rat liver against DOX-induced injury by inhibiting DOX-induced oxidative stress, fibrotic changes, tissue inflammation, and apoptosis. The pregnenolone-mediated hepatoprotection involves activating endogenous antioxidant mechanisms, upregulating Nrf2/HO-1 and P-gp, and mitigating inflammation by antagonizing NFκB signaling. Importantly, pregnenolone did not antagonize the anticancer effects of DOX in liver cancer cells but rather potentiated it. Thus, combining pregnenolone and DOX might offer better therapeutic outcomes, fewer DOX-induced adverse effects, and better compliance.

Data Availability
Data are contained within the article or available upon reasonable request from the corresponding author.

Conflicts of Interest
The authors declare no conflict of interest.

Ethics Approval
The experimental protocol was approved by the Institutional Research Ethics Committee of Faculty of Medicine, Minia University (Approval No. 717:12/2020).

Informed Consent
Not applicable.

Funding
This research was funded by King Abdulaziz City of Science and Technology (KACST), Saudi Arabia (Grant No. 12-MED3156-06).

Authors' Contributions
M.A.M., M.E. and S.A.A. designed the experimental project. M.A.M., M.E., B.A.K., R.A.R. and S.A.A. contributed to acquiring, analyzing, and interpreting the data. M.A.M., M.E., R.A.R. and S.A.A. wrote, reviewed, and edited the manuscript. M.A.M supervised and provided funding. Finally, all contributing authors have read and approved the submitted manuscript.

Acknowledgements
We are thankful to the King Abdulaziz City of Science and Technology (KACST), Saudi Arabia, for their financial support by grant No. 12-MED3156-06.

ORCID ID
M.A. Morsy: 0000-0002-6752-9094
M. El-Daly: 0000-0001-5971-1104
B.A. Kamel: 0000-0001-8479-7720
R.A. Rifaai: 0000-0002-7481-2656
S.A. Abdel-Gaber: 0000-0003-1755-0837

References

1) Gadducci A, Cosio S. Trabectedin and lurbinectedin: Mechanisms of action, clinical impact, and future perspectives in uterine and soft tissue sarcoma, ovarian carcinoma, and endometrial carcinoma. Front Oncol 2022; 12: 914342.
2) Wu T, Wu Y, Chen S, Wu J, Zhu W, Liu H, Chen M, Xu B. Curative Effect and Survival Assessment Comparing Gemcitabine and Cisplatin Versus Methotrexate, Vinblastine, Doxorubicin and Cisplatin as Neoadjuvant Therapy for Bladder Cancer: A Systematic Review and Meta-Analysis. Front Oncol 2021; 11: 678896.
3) Chen H, Pan T, He Y, Zeng R, Li Y, Yi L, Zang H, Chen S, Duan Q, Xiao L, Zhou H. Primary Mediastinal B-Cell Lymphoma: Novel Precision Therapies and Future Directions. Front Oncol 2021; 11: 654854.
4) Sparano JA, Lee JY, Kaplan LD, Ramos JC, Ambinder RF, Wachsman W, Aboulafia D, Noy A, Henry DH, Ratner L, Cesarman E, Chadburn A, Mitsuyasu R. Response-adapted therapy with infusional EPOCH chemotherapy plus rituximab in HIV-associated, B-cell non-Hodgkin's lymphoma. Haematologica 2021; 106: 730-735.
5) Bagdasaryan AA, Chubarev VN, Smolyarchuk EA, Drozdov VN, Krasnyuk II, Liu J, Fan R, Tse E, Shikh EV, Sukocheva OA. Pharmacogenetics of Drug Metabolism: The Role of Gene Polymorphism in the Regulation of Doxorubicin Safety and Efficacy. Cancers 2022; 14: 5436.
6) Huang KM, Zavorka Thomas M, Magdy T, Eisenmann ED, Uddin ME, Digiacomo DF, Pan A, Keiser M, Otter M, Xia SH. Targeting OCT3 attenuates doxorubicin-induced cardiac injury. Proc Natl Acad Sci U S A 2021; 118: e2020168118.
7) Sirwi A, Shaik RA, Alamoudi AJ, Eid BG, Kammoun AK, Ibrahim SRM, Mohamed GA, Abdallah HM, Abdel-Naim AB. Mokko Lactone Attenuates Doxorubicin-Induced Hepatotoxicity in Rats: Emphasis on Sirt-1/FOXO1/NF-κB Axis. Nutrients 2021; 13: 4142.
8) Chen X, Zhang Y, Zhu Z, Liu H, Guo H, Xiong C, Xie K, Zhang X, Su S. Protective effect of berberine on doxorubicin-induced acute hepatorenal toxicity in rats. Mol Med Rep 2016; 13: 3953-3960.

9) Licata S, Saponiero A, Mordente A, Minotti G. Doxorubicin metabolism and toxicity in human myocardium: role of cytoplasmic deglycosidation and carbonyl reduction. Chem Res Toxicol 2000; 13: 414-420.
10) Saleh DO, Mahmoud SS, Hassan A, Sanad EF. Doxorubicin-induced hepatic toxicity in rats: Mechanistic protective role of Omega-3 fatty acids through Nrf2/HO-1 activation and PI3K/Akt/GSK-3beta axis modulation. Saudi J Biol Sci 2022; 29: 103308.
11) Wang YC, Wang LT, Hung TI, Hong YR, Chen CH, Ho CJ, Wang C. Severe cellular stress drives apoptosis through a dual control mechanism independently of p53. Cell Death Discov 2022; 8: 282.
12) Rawat PS, Jaiswal A, Khurana A, Bhatti JS, Navik U. Doxorubicin-induced cardiotoxicity: An update on the molecular mechanism and novel therapeutic strategies for effective management. Biomed Pharmacother 2021; 139: 111708.
13) Matouk AI, El-Daly M, Habib HA, Senousy S, Naguib Abdel Hafez SM, Kasem AW, Almalki WH, Alzahrani A, Alshehri A, Ahmed AF. Protective effects of menthol against sepsis-induced hepatic injury: Role of mediators of hepatic inflammation, apoptosis, and regeneration. Front Pharmacol 2022; 13: 952337.
14) Morsy MA, Younis NS, El-Sheikh AaK, Al Turaifi FH, El-Daly M, Mohafez OM. Protective mechanisms of piperine against acetaminophen-induced hepatotoxicity may be mediated through TGFBRAP1. Eur Rev Med Pharmacol Sci 2020; 24: 10169-10180.
15) Liao W, Rao Z, Wu L, Chen Y, Li C. Cariporide Attenuates Doxorubicin-Induced Cardiotoxicity in Rats by Inhibiting Oxidative Stress, Inflammation and Apoptosis Partly Through Regulation of Akt/GSK-3β and Sirt1 Signaling Pathway. Front Pharmacol 2022; 13: 850053.
16) Teng S, Piquette-Miller M. The involvement of the pregnane X receptor in hepatic gene regulation during inflammation in mice. J Pharmacol Exp Ther 2005; 312: 841-848.
17) Shah YM, Ma X, Morimura K, Kim I, Gonzalez FJ. Pregnane X receptor activation ameliorates DSS-induced inflammatory bowel disease via inhibition of NF-kappaB target gene expression. Am J Physiol Gastrointest Liver Physiol 2007; 292: G1114-1122.
18) Grigoreva TA, Sagaidak AV, Novikova DS, Tribulovich VG. Implication of ABC transporters in non-proliferative diseases. Eur J Pharmacol 2022; 935: 175327.
19) Modi A, Roy D, Sharma S, Vishnoi JR, Pareek P, Elhence P, Sharma P, Purohit P. ABC transporters in breast cancer: their roles in multidrug resistance and beyond. J Drug Target 2022; 30: 927-947.
20) El-Sayed WM. Effect of pregnane X receptor (PXR) prototype agonists on chemoprotective and drug metabolizing enzymes in mice. Eur J Pharmacol 2011; 660: 291-297.
21) Sun L, Sun Z, Wang Q, Zhang Y, Jia Z. Role of nuclear receptor PXR in immune cells and inflammatory diseases. Front Immunol 2022; 13: 969399.
22) Lv C, Huang L. Xenobiotic receptors in mediating the effect of sepsis on drug metabolism. Acta Pharm Sin B 2020; 10: 33-41.
23) Wang Q, Song GC, Weng FY, Zou B, Jin JY, Yan DM, Tan B, Zhao J, Li Y, Qiu FR. Hepatoprotective Effects of Glycyrrhetinic Acid on Lithocholic Acid-Induced Cholestatic Liver Injury Through Choleretic and Anti-Inflammatory Mechanisms. Front Pharmacol 2022; 13: 881231.
24) Okamura M, Shizu R, Abe T, Kodama S, Hosaka T, Sasaki T, Yoshinari K. PXR Functionally Interacts with NF-κB and AP-1 to Downregulate the Inflammation-Induced Expression of Chemokine CXCL2 in Mice. Cells 2020; 9: 2296.
25) Kodama S, Shimura T, Kuribayashi H, Abe T, Yoshinari K. Pregnenolone 16α-carbonitrile ameliorates concanavalin A-induced liver injury in mice independent of the nuclear receptor PXR activation. Toxicol Lett 2017; 271: 58-65.
26) Lejri I, Grimm A, Hallé F, Abarghaz M, Klein C, Maitre M, Schmitt M, Bourguignon JJ, Mensah-Nyagan AG, Bihel F. TSPO ligands boost mitochondrial function and pregnenolone synthesis. J Alzheimers Dis 2019; 72: 1045-1058.
27) Andrabi SS, Kaushik P, Mumtaz SM, Alam MM, Tabassum H, Parvez S. Pregnenolone Attenuates the Ischemia-Induced Neurological Deficit in the Transient Middle Cerebral Artery Occlusion Model of Rats. ACS Omega 2022; 7: 19122-19130.
28) Layton C, Bancroft JD, Suvarna SK. 4 - Fixation of tissues, in Bancroft's Theory and Practice of Histological Techniques (Eighth Edition). Elsevier, 2019; 40-63.
29) Senousy SR, Ahmed AF, Abdelhafeez DA, Khalifa MMA, Abourehab MAS, El-Daly M. Alpha-Chymotrypsin Protects Against Acute Lung, Kidney, and Liver Injuries and Increases Survival in CLP-Induced Sepsis in Rats Through Inhibition of TLR4/NF-κB Pathway. Drug Des Devel Ther 2022; 16: 3023-3039.
30) Al-Kadi A, El-Daly M, El-Tahawy NFG, Khalifa MMA, Ahmed A-SF. Angiotensin aldosterone inhibitors improve survival and ameliorate kidney injury induced by sepsis through suppression of inflammation and apoptosis. Fundam Clin Pharmacol 2022; 36: 286-295.
31) Refaie MMM, Abdel-Gaber SA, Rahman S, Hafez S, Khalaf HM. Cardioprotective effects of bosentan in 5-fluorouracil-induced cardiotoxicity. Toxicology 2022; 465: 153042.
32) Morsy MA, Gupta S, Nair AB, Venugopala KN, Greish K, El-Daly M. Protective Effect of Spirulina platensis Extract against Dextran-Sulfate-Sodium-Induced Ulcerative Colitis in Rats. Nutrients 2019; 11: 2309.
33) Morsy MA, El-Sheikh AaK, Abdel-Hafez SMN, Kandeel M, Abdel-Gaber SA. Paeonol Protects Against Methotrexate-Induced Nephrotoxicity via Upregulation of P-gp Expression and Inhibition of TLR4/NF-κB Pathway. Front Pharmacol 2022; 13: 774387.
34) Raafat M, Kamel AA, Shehata AH, Ahmed AF, Bayoumi AMA, Moussa RA, Abourehab MaS, El-Daly M. Aescin Protects against Experimental Benign Prostatic Hyperplasia and Preserves Prostate Histomorphology in Rats via Suppression of Inflammatory Cytokines and COX-2. Pharmaceuticals (Basel) 2022; 15: 130.

35) Schneider CA, Rasband WS, Eliceiri KW. NIH Image to ImageJ: 25 years of image analysis. Nat Methods 2012; 9: 671-675.
36) Bancroft JD, Layton C. 12 - Connective and other mesenchymal tissues with their stains, in Bancroft's Theory and Practice of Histological Techniques (Eighth Edition). Elsevier, 2019; 153-175.
37) Cao S, Zheng B, Chen T, Chang X, Yin B, Huang Z, Shuai P, Han L. Semen Brassicae ameliorates hepatic fibrosis by regulating transforming growth factor-β1/Smad, nuclear factor-κB, and AKT signaling pathways in rats. Drug Des Devel Ther 2018; 12: 1205-1213.
38) Ahmed OM, Elkomy MH, Fahim HI, Ashour MB, Naguib IA, Alghamdi BS, Mahmoud HUR, Ahmed NA. Rutin and Quercetin Counter Doxorubicin-Induced Liver Toxicity in Wistar Rats via Their Modulatory Effects on Inflammation, Oxidative Stress, Apoptosis, and Nrf2. Oxid Med Cell Longev 2022; 2022: 2710607.
39) Barakat BM, Ahmed HI, Bahr HI, Elbahaie AM. Protective Effect of Boswellic Acids against Doxorubicin-Induced Hepatotoxicity: Impact on Nrf2/HO-1 Defense Pathway. Oxid Med Cell Longev 2018; 2018: 8296451.
40) Prasanna PL, Renu K, Valsala Gopalakrishnan A. New molecular and biochemical insights of doxorubicin-induced hepatotoxicity. Life Sci 2020; 250: 117599.
41) Ma Y, North BJ, Shu J. Regulation of topoisomerase II stability and activity by ubiquitination and SUMOylation: clinical implications for cancer chemotherapy. Mol Biol Rep 2021; 48: 6589-6601.
42) Wang D, Tang L, Zhang Y, Ge G, Jiang X, Mo Y, Wu P, Deng X, Li L, Zuo S, Yan Q, Zhang S, Wang F, Shi L, Li X, Xiang B, Zhou M, Liao Q, Guo C, Zeng Z, Xiong W, Gong Z. Regulatory pathways and drugs associated with ferroptosis in tumors. Cell Death Dis 2022; 13: 544.
43) Song S, Chu L, Liang H, Chen J, Liang J, Huang Z, Zhang B, Chen X. Protective Effects of Dioscin Against Doxorubicin-Induced Hepatotoxicity Via Regulation of Sirt1/FOXO1/NF-kappab Signal. Front Pharmacol 2019; 10: 1030.
44) Zhou Z, Qi J, Zhao J, Seo JH, Shin DG, Cha JD, Lim CW, Kim JW, Kim B. Orostachys japonicus ameliorates acetaminophen-induced acute liver injury in mice. J Ethnopharmacol 2021; 265: 113392.
45) Jiang Q, Chen X, Tian X, Zhang J, Xue S, Jiang Y, Liu T, Wang X, Sun Q, Hong Y, Li C, Guo D, Wang Y, Wang Q. Tanshinone I inhibits doxorubicin-induced cardiotoxicity by regulating Nrf2 signaling pathway. Phytomedicine 2022; 106: 154439.
46) Nordgren KKS, Wallace KB. Keap1 redox-dependent regulation of doxorubicin-induced oxidative stress response in cardiac myoblasts. Toxicol Appl Pharmacol 2014; 274: 107-116.
47) Nordgren KKS, Wallace KB. Disruption of the Keap1/Nrf2-Antioxidant Response System After Chronic Doxorubicin Exposure In Vivo. Cardiovasc Toxicol 2020; 20: 557-570.
48) Alasmari AF, Alharbi M, Alqahtani F, Alasmari F, Alswayyed M, Alzarea SI, Al-Alallah IA, Alghamdi A, Hakami HM, Alyousef MK. Diosmin Alleviates Doxorubicin-Induced Liver Injury via Modulation of Oxidative Stress-Mediated Hepatic Inflammation and Apoptosis via NfkB and MAPK Pathway: A Preclinical Study. Antioxidants 2021; 10: 1998.
49) Xu X, Liu Q, Li J, Xiao M, Gao T, Zhang X, Lu G, Wang J, Guo Y, Wen P, Gu J. Co-Treatment With Resveratrol and FGF1 Protects Against Acute Liver Toxicity After Doxorubicin Treatment via the AMPK/NRF2 Pathway. Front Pharmacol 2022; 13: 940406.
50) Zhao X, Jin Y, Li L, Xu L, Tang Z, Qi Y, Yin L, Peng J. MicroRNA-128-3p aggravates doxorubicin-induced liver injury by promoting oxidative stress via targeting Sirtuin-1. Pharmacol Res 2019; 146: 104276.
51) Kabel AM, Alzahrani AA, Bawazir NM, Khawtani RO, Arab HH. Targeting the proinflammatory cytokines, oxidative stress, apoptosis and TGF-beta1/STAT-3 signaling by irbesartan to ameliorate doxorubicin-induced hepatotoxicity. J Infect Chemother 2018; 24: 623-631.
52) Henry BM, Benoit SW, Vikse J, Berger BA, Pulvino C, Hoehn J, Rose J, Santos De Oliveira MH, Lippi G, Benoit JL. The anti-inflammatory cytokine response characterized by elevated interleukin-10 is a stronger predictor of severe disease and poor outcomes than the pro-inflammatory cytokine response in coronavirus disease 2019 (COVID-19). Clin Chem Lab Med 2021; 59: 599-607.
53) Huang G, Hua S, Liu H, Zhou H, Chen X, Wang Z, Yu W. Efficacy of ifosfamide combined with liposome doxorubicin on osteosarcoma and its effects on serum IL-10, TNF-α, and IFN-γ in patients with osteosarcoma. Am J Transl Res 2022; 14: 1288-1296.
54) Al-Qahtani WH, Alshammari GM, Ajarem JS, Al-Zahrani AY, Alzuwaydi A, Eid R, Yahya MA. Isoliquiritigenin prevents Doxorubicin-induced hepatic damage in rats by upregulating and activating SIRT1. Biomed Pharmacother 2022; 146: 112594.
55) Beyer C, Skapenko A, Distler A, Dees C, Reichert H, Munoz L, Leipe J, Schulze-Koops H, Distler O, Schett G, Distler JH. Activation of pregnane X receptor inhibits experimental dermal fibrosis. Ann Rheum Dis 2013; 72: 621-625.
56) Amer AO, Probert PM, Dunn M, Knight M, Vallance AE, Flecknell PA, Oakley F, Cameron I, White SA, Blain PG, Wright MC. Sustained Isoprostane E2 Elevation, Inflammation and Fibrosis after Acute Ischaemia-Reperfusion Injury Are Reduced by Pregnane X Receptor Activation. PLoS One 2015; 10: e0136173.
57) Leskiewicz M, Regulska M, Budziszewska B, Jantas D, Jaworska-Feil L, Basta-Kaim A, Kubera M, Jagla G, Nowak W, Lason W. Effects of neurosteroids on hydrogen peroxide- and staurosporine-induced damage of human neuroblastoma SH-SY5Y cells. J Neurosci Res 2008; 86: 1361-1370.
58) Beilke LD, Aleksunes LM, Olson ER, Besselsen DG, Klaassen CD, Dvorak K, Cherrington NJ. Decreased apoptosis during CAR-mediated hepatoprotection against lithocholic acid-induced liver injury in mice. Toxicol Lett 2009; 188: 38-44.
59) Elhinnawi MA, Mohareb RM, Rady HM, Khalil WKB, Abd Elhalim MM, Elmegeed GA. Novel pregnenolone derivatives modulate apoptosis via Bcl-2 family genes in hepatocellular carcinoma in vitro. J Steroid Biochem Mol Biol 2018; 183: 125-136.

60) Cascio C, Guarneri R, Russo D, De Leo G, Guarneri M, Piccoli F, Guarneri P. A caspase-3-dependent pathway is predominantly activated by the excitotoxin pregnenolone sulfate and requires early and late cytochrome c release and cell-specific caspase-2 activation in the retinal cell death. J Neurochem 2002; 83: 1358-1371.
61) Ma EL, Zhao DM, Li YC, Cao H, Zhao QY, Li JC, Sun LX. Activation of ATM-Chk2 by 16-dehydropregnenolone induces G1 phase arrest and apoptosis in HeLa cells. J Asian Nat Prod Res 2012; 14: 817-825.
62) Xiao X, Chen L, Ouyang Y, Zhu W, Qiu P, Su X, Dou Y, Tang L, Yan M, Zhang H, Yang X, Xu D, Yan G. Pregnenolone, a cholesterol metabolite, induces glioma cell apoptosis via activating extrinsic and intrinsic apoptotic pathways. Oncol Lett 2014; 8: 645-650.
63) Ibrahim YF, Moussa RA, Bayoumi AMA, Ahmed A-SF. Tocilizumab attenuates acute lung and kidney injuries and improves survival in a rat model of sepsis via down-regulation of NF-κB/JNK: a possible role of P-glycoprotein. Inflammopharmacology 2020; 28: 215-230.